

## Preparation and Characterization of Poly(vinyl chloride)/Polystyrene/Poly(ethylene glycol) Hollow-Fiber Ultrafiltration Membranes

Qusay Alsally,<sup>1</sup> Amil Merza,<sup>2</sup> Khalid Rashid,<sup>1</sup> Arman Adam,<sup>2</sup> Alberto Figoli,<sup>3</sup>  
 Silvia Simone,<sup>3</sup> Enrico Drioli<sup>3,4</sup>

<sup>1</sup>Chemical Engineering Department, University of Technology, Alsinaa Street Number 52, Baghdad, Iraq

<sup>2</sup>Technical College, Alzufrania, Baghdad, Iraq

<sup>3</sup>Institute of Membrane Technology, University of Calabria, 87030, Rende CS (Cosenza), Italy

<sup>4</sup>Department of Chemical Engineering and Materials, University of Calabria, 87030, Rende CS (Cosenza), Italy

Correspondence to: Q. Alsally (E-mail: qusayalsally@uotechnology.edu.iq or qusay\_alsally@yahoo.com)

**ABSTRACT:** Hollow-fiber ultrafiltration (UF) membranes were prepared from blends of poly(vinyl chloride) (PVC) and polystyrene (PS) with a dry/wet phase inversion method. Poly(ethylene glycol) (PEG) and *N,N*-dimethylacetamide were used as the additive and solvent, respectively. The effects of the PEG concentration in the dope solution as an additive on the cross sections and inner and outer surface morphologies, permeability, and separation performance of the hollow fibers were examined. The mean pore size, pore size distribution, and mean roughness of both the inner and outer surfaces of the produced hollow fibers were determined by atomic force microscopy. Also, the mechanical properties of the hollow-fiber membranes were investigated. UF experiments were conducted with aqueous solutions of poly(vinyl pyrrolidone) (PVP; K-90,  $M_w = 360$  kDa). From the results, we found that the PVC/PS hollow-fiber membranes had two layers with a fingerlike structure. These two layers were changed from a wide and long to a thin and short morphology with increasing PEG concentration. A novel and until now undescribed shape of the nodules in the outer surfaces, which was denoted as a sea-waves shape, was observed. The outer and inner pore sizes both increased with increasing PEG concentration. The water permeation flux of the hollow fibers increased from 104 to 367 L m<sup>-2</sup> h<sup>-1</sup> bar<sup>-1</sup> at higher PEG concentrations. The PVP rejection reached the highest value at a PEG concentration of 4 wt %, whereas at higher values (from 4 to 9 wt %), the rejection decreased. The same trend was found also for the tensile stress at break, Young's modulus, and elongation at break of the hollow fibers. © 2013 Wiley Periodicals, Inc. *J. Appl. Polym. Sci.* 130: 989–1004, 2013

**KEYWORDS:** blends; membranes; morphology; poly(vinyl chloride); properties and characterization

Received 9 August 2012; accepted 25 February 2013; Published online 17 April 2013

DOI: 10.1002/app.39221

### INTRODUCTION

The blending of two different polymers offers attractive opportunities for the development of novel materials with valuable combinations of properties that can also be modulated by the addition of a third, water-soluble component.

In particular, in a previous study,<sup>1</sup> ultrafiltration (UF) hollow-fiber membranes were prepared by the blending of poly(vinyl chloride) (PVC) (14 wt %) and polystyrene (PS; 0–6 wt %). It was found that the fiber morphology was affected by the PS concentration. Water permeability was not decreased by the addition of 1–2 wt % PS, whereas interestingly, the rejection (*R*) to poly(vinyl pyrrolidone) (PVP) K-90 ( $M_w = 360$  kDa) increased from 76.2 to 98.53% with the addition of 1 wt % PS to the dope solution. The addition of PS was also found to improve the fiber mechanical properties.

Furthermore, the membrane morphology could be modulated by the addition of water-soluble additives, such as poly(ethylene glycol) (PEG) and PVP in the dope solution to improve the membrane morphology and performance.<sup>2–11</sup> For instance, Kim and Lee<sup>2</sup> investigated the effects of the PEG molecular weight and concentration (PEG was a pore former) on the morphology and permeation properties of polysulfone/*N*-methyl-2-pyrrolidone (NMP)/PEG membranes connected with the changes in the thermodynamic and kinetic properties in the phase-inversion process. Xu and Alsally<sup>4</sup> fabricated poly(ether sulfone) hollow-fiber membranes with PEG with different molecular weights (PEG-200, PEG-600, PEG-2000, PEG-6000, and PEG-10000) and PVP-40000 as additives and NMP as the solvent. They found that with an increase in the PEG molecular weight from 200 to 10,000 in the dope solution, the membrane structures were changed, and the pure water permeation fluxes

**Table I.** Compositions of the Dope Solutions and Spinning Conditions of the PVC Hollow-Fiber Membranes Produced in This Study

Fiber number	Polymer solution (wt %)				Outer and inner coagulant temperature (°C)	Air gap (cm)	Extrusion pressure (bar)	Bore fluid	Bore flow rate (mL/min)
	PVC	PS	DMAc	PEG					
M0-0	16	0	84	0	30 ± 1	4	1.5	Water	0.4
M1-0	16	1	83	0	30 ± 1	4	1.5	Water	0.4
M1-2	16	1	81	2	30 ± 1	4	1.5	Water	0.4
M1-3	16	1	80	3	30 ± 1	4	1.5	Water	0.4
M1-4	16	1	79	4	30 ± 1	4	1.5	Water	0.4
M1-7	16	1	76	7	30 ± 1	4	1.5	Water	0.4
M1-9	16	1	74	9	30 ± 1	4	1.5	Water	0.4

improved. Chou et al.<sup>6</sup> prepared asymmetric cellulose acetate hollow-fiber membranes by a dry/wet-spinning process with PEG as an additive. They showed that the addition of PEG suppressed the formation of macrovoids, particularly for PEG with a higher molecular weight and concentration. They also found that the pure water permeation flux increased with PEG concentration. Wongchitphimon et al.<sup>8</sup> studied the effects of PEG with different molecular weights and different loadings as an additive on the fabrication of polyvinylidene fluoride-co-hexafluoropropylene (PVDF-HFP) asymmetric microporous hollow-fiber membranes. Their experiments revealed that the addition of PEG to the PVDF-HFP/NMP solution resulted in a thermodynamically less stable system in reaction with water; this promoted rapid-phase demixing in the phase-inversion process. The pure water permeability (PWP) increased accordingly.

Finally, Simone et al.<sup>11</sup> investigated the combined effect of water and PVP on the morphology and vacuum membrane distillation (VMD) performance of PVDF hollow-fiber membranes. They found that the membrane morphology was affected by the PVP concentration as a result of the two different effects. On one side, an increase in the PVP concentration promoted the formation of macrovoids because of the hydrophilic characteristics of this polymer, which promoted a faster liquid/liquid demixing rate (a thermodynamic effect). On the other hand, at higher PVP concentrations, the increased dope viscosity delayed the liquid/liquid demixing process and thus promoted the formation of spongelike structures (a kinetic effect).

With regard to the polymer used in this study, several studies have reported the preparation of membranes from PVC as a polymer material.<sup>12–14</sup> For example, Peng and Sui,<sup>12</sup> reported that the hydrophilicity of the PVC membrane increased by addition of poly(vinyl butyral) (PVB) as the second polymer. The water permeation flux and hydrophilicity of the blended membranes were improved with respect to membranes prepared from neat PVC or PVB. In a previous work, Khayet et al.<sup>13</sup> prepared PVC hollow-fiber membranes with different air-gap distances. It was concluded that with small air-gap distances, the membrane properties and performance were highly improved. Moreover, PVC gas-separation hollow-fiber membranes were produced from multicomponent dopes with dry/wet forced convection spinning by Jones et al.<sup>14</sup> However, membranes spun

from a low-polymer-content solution exhibited disappointing gas-separation properties, whereas the preliminary test indicated that the membranes prepared with a high polymer concentration were capable of achieving a degree of separation for the O<sub>2</sub>/O<sub>3</sub> system.

In this study, the PVC/PS blend hollow-fiber membranes were prepared with 1 wt % PS with a dry/wet phase inversion method. The effect of the PEG concentration ( $M_w = 4000$  Da) in the dope solution as a pore former on the structural morphology of the PVC/PS blend hollow-fiber membrane was studied by means of a scanning electron microscopy (SEM) technique and atomic force microscopy (AFM). The performance of the produced hollow-fiber membranes was investigated by water permeation and the poly(vinyl pyrrolidone) (PVP) K-90 ( $M_w = 360$  KDa) *R* behavior. The hollow-fiber mechanical properties were determined by the measurement of the membrane's tensile strength ( $R_m$ ) at break, Young's modulus (EMod), and elongation at break (ebreak).

## EXPERIMENTAL

### Materials

PVC resins in powder form, with an average degree of polymerization of 1040 ( $M_w = 65,000$  Da), supplied by Georgia Gulf Co., and PS ( $M_w = 286,000$  Da) were used as membrane materials. *N,N*-Dimethylacetamide (DMAc), supplied by Sigma Aldrich Co., was used as a solvent. PEG, with a  $M_w$  of 4000 Da, was supplied by Fluka Co. and was used as an additive. PVP K-90 ( $M_w = 360$  kDa (Fluka Co.)) was used as solute for performing *R* tests.

### Preparation of the Polymer Dope Solution

PVC powder and PS were dried separately in an oven for about 2 h at 70°C to remove residual moisture. DMAc was put in a dry glass flask. Dried 1 wt % PS was added gradually to the solvent; then, different percentages (0–9 wt %) of PEG-4000 were added with continuous mixing by a magnetic stirrer until the dope became homogeneous. Dried 16 wt % PVC was then gradually added to the PS/DMAc solution under continuous mixing by a magnetic stirrer. The glass flask was closed perfectly (to prevent any amount of moisture from the atmosphere from contacting the dope solution). The dope was left under mixing at 35°C until it became homogeneous, usually within 3 days. The dope was then allowed to de-gas before spinning.

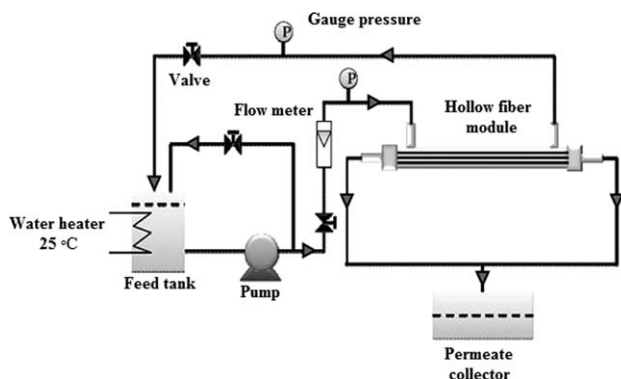


**Figure 1.** Schematic diagram of the UF setup used for measurements of PWP and *R* (%).

### PVC/PS/PEG Hollow-Fiber Spinning Methods

The PVC/PS hollow-fiber membranes were spun at room temperature with the dry/wet-spinning method as described elsewhere<sup>1</sup> with a tube-in-orifice spinneret (i.d./o.d. = 500/900 μm).

Table I summarizes the composition and spinning conditions of the fabricated PVC/PS/PEG hollow-fiber membranes. The PEG concentration in the dope solution was varied from 0 to 9 wt %, and all of the other spinning conditions were kept constant. The ratio of the dope solution flow rate to the bore fluid flow rate was constant in all of the spinning processes. All of the nascent fibers were undrawn (free falling velocity); that is, the take-up velocity was nearly the same as the falling velocity in the coagulation bath. The coagulation bath and bore fluid were maintained at 30°C. The fabricated PVC/PS/PEG hollow fibers were rinsed with water to eliminate the residual solvent and treated with glycerol (30 wt %) to prevent any collapse of their porous structure, as already described in previous articles.<sup>15,16</sup> The fibers were finally dried in air at room temperature before the preparation of modules for UF tests.

### Measurements of the Membrane Dimensions

The i.d. and o.d. values of the prepared PVC/PS/PEG hollow fibers were measured with a linear vernier microscope (Griffin) with a precision of ±0.01 mm.

### SEM Observations

The fiber cross sections and inner and outer surface morphologies were observed with a scanning electron microscope (Quanta FENG 200, FEI Co., Hillsboro, OR, provided by University of

Calabria, Italy). Fiber cross sections were prepared with liquid nitrogen to obtain a clean brittle fracture.

### AFM Characterization of the Hollow-Fiber Membrane Surface

Each hollow fiber was subjected to extensive surface analysis with AFM (model AA3000, Angstrom Advanced, Inc.). A contact mode with a suitable silicon tip was used to estimate the topography (the rise and fall of the sample surface), lateral force (friction forces between the tip and sample, which caused the torsion of the cantilever and could be reflected by the photodetector's left–right signal), deflection (the cantilever flexed because of the rise and fall of the sample topography, and the amount of this deflection could be reflected by the photodetector's up–down signal). With IMAGER 4.31 software, a statistical pore size distribution was established for the outer and inner surfaces of each hollow fiber.

### Mechanical Properties

The  $R_{mp}$ , ebreak, and EMod values of the produced PVC/PS/PEG fibers were measured as described in previous works<sup>15,16</sup> by means of a Zwick/Roell Z 2.5 test unit.

### Porosity Measurements

The membrane porosity ( $\epsilon_m$ ) can be defined as the void fraction, that is, the volume of the pores divided by the total volume of the membrane. It was determined by the gravimetric method, as described in the literature.<sup>17</sup> Briefly, hollow fibers not previously treated with the glycerol solution were dried and weighed with a precision balance. The fibers were then immersed in kerosene for 24 h; the excess liquid was wiped away with tissue paper, and the fibers were weighed again. The overall  $\epsilon_m$  was calculated according to the following formula:

$$\epsilon_m(\%) = \frac{[(W_1 - W_2)/D_{\text{Kerosene}}]}{[(W_1 - W_2)/D_{\text{Kerosene}} + W_2/D_{\text{Polymer}}]} \times 100 \quad (1)$$

where  $W_1$  is the weight of the wet membrane,  $W_2$  is the weight of the dry membrane,  $D_{\text{Kerosene}}$  is the kerosene density (0.82 g/cm<sup>3</sup>), and  $D_{\text{Polymer}}$  is the PVC/PS density (1.379 cm<sup>3</sup>)<sup>18</sup>.

### Preparation of the Hollow-Fiber Membrane Modules

For the preparation of the hollow-fiber modules, five fibers were coaxially inserted into a stainless steel tube sealed at both extremities by epoxy glue. The modules were left overnight to cure as described in previous works.<sup>15,16</sup>

### Measurements of the Permeation Flux and Solute *R*

A schematic diagram of the UF experiments setup is presented in Figure 1. Before each test, hollow-fiber modules were immersed in distilled water for 24 h and run in the test system for 1.5 h to

**Table II.** PVC/PS/PEG Hollow-Fiber Membrane Dimensions and Porosity

Fiber number	o.d. (mm)	i.d. (mm)	Thickness (mm)	Porosity
M0-0	1.19 ± 0.01	0.58 ± 0.01	0.31 ± 0.01	87.88 ± 0.33
M1-0	1.19 ± 0.05	0.64 ± 0.02	0.28 ± 0.04	84.37 ± 0.38
M1-2	1.08 ± 0.03	0.64 ± 0.03	0.22 ± 0.03	83.42 ± 0.22
M1-3	1.11 ± 0.07	0.57 ± 0.05	0.27 ± 0.06	82.90 ± 0.17
M1-4	1.09 ± 0.05	0.56 ± 0.03	0.27 ± 0.04	83.30 ± 0.65
M1-7	1.10 ± 0.02	0.83 ± 0.03	0.14 ± 0.02	83.35 ± 0.61
M1-9	1.16 ± 0.07	0.91 ± 0.06	0.13 ± 0.06	83.55 ± 0.96

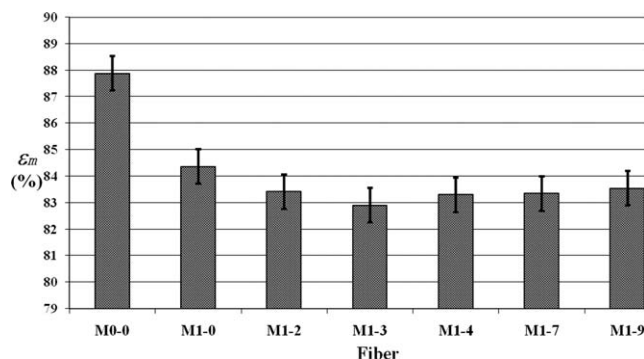


**Figure 2.** Effect of the PEG concentration on  $\epsilon_m$  (%) of the PVC hollow-fiber membranes produced in this study.

eliminate the effect of the residual glycerol. For each hollow-fiber type, three modules were prepared, and the duration of the performance test for each sample was 2 h. The PWP was calculated with the following formula:

$$J_w = \frac{Q_w}{\Delta P A_s} \quad (2)$$

where  $J_w$  is the pure water permeability of the membrane ( $\text{L m}^{-2} \cdot \text{h}^{-1} \cdot \text{bar}^{-1}$ ),  $Q_w$  is the volumetric flow rate (L/h),  $\Delta P$  is the transmembrane pressure drop (bar), and  $A_s$  is the membrane surface area ( $\text{m}^2$ ) calculated on the basis of the fiber number, effective length, and o.d. (UF tests were performed with the outside/in configuration). A concentration of 1000 ppm of PVP K-90 ( $M_w = 360$  kDa) was used to determine the PVC/PS/PEG hollow-fiber membrane  $R$  (%), which was calculated as follows:

$$R(\%) = \left(1 - \frac{C_p}{C_f}\right) \times 100\% \quad (3)$$

where  $C_f$  and  $C_p$  are the solute concentrations in the feed and permeate solution, respectively. The concentration of PVP was calculated on the basis of a calibration curve of optical density versus concentration determined by a UV spectrophotometer (Shimadzu UV160 A, Japan) at wavelength of 212 nm.

## RESULTS AND DISCUSSION

### Effect of the PEG Concentration on the Dimensions and Porosity

The membrane characteristics (i.d., o.d., thickness and porosity) of the PVC/PS hollow fibers prepared under different PEG concentrations in dope solution are summarized in Table II. The fiber o.d. was not much affected by the PEG concentration. The similarity in the o.d. values of the PVC/PS/PEG hollow fibers could be explained by the used air-gap distance. As observed in a previous study,<sup>15</sup> when air gap as short as 4 cm was used, there was not sufficient time for the die swell of the polymeric dope to be triggered. It was observed that this air-gap distance could eliminate the effect of the PVC concentration on the fiber dimensions. In that case, the o.d. of the produced PVC hollow-fiber membranes was nearly the same as that of the spinneret (0.9 mm). In this case, however, the fiber o.d. values were slightly bigger than those of the spinneret. This could be attributed to the higher temperature ( $T$ ) of the coagulation bath used in this study ( $T = 30^\circ\text{C}$ ). Similar behavior was also observed in

a previous study with a PVC/PS blend:<sup>1</sup> an air-gap distance of 5 cm was able to overcome the effect of the PS concentration in the dope solution on the hollow-fiber membrane dimensions.

The i.d. of the PVC/PS/PEG hollow-fiber membranes decreased from 0.64 to 0.56 mm for the PVC hollow-fiber membranes prepared with 1 wt % PS and a PEG concentration increasing from 0 to 4 wt % (from M1-0 to M1-4). In contrast, the i.d. gradually increased up to 0.91 mm at higher PEG concentrations in the dope solution from 4 to 9 wt % (from M1-4 to M1-9).

The decrease and increase the fiber i.d. with PEG concentration could be attributed to the superposition of thermodynamic and kinetic effects during fiber coagulation. PEG is a hydrophilic additive. A low PEG concentration in the dope solution enhanced the nonsolvent inflow from the bore fluid to the fiber inner layer (a thermodynamic effect). Therefore, at low PEG concentrations, the coagulation of the hollow-fiber inner surface

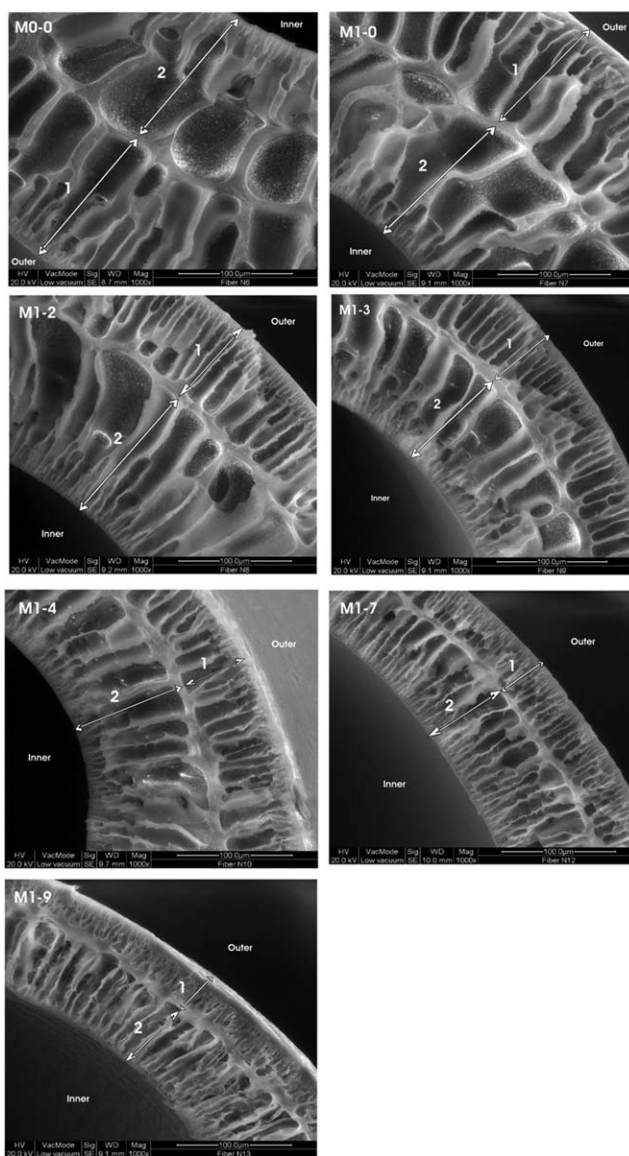


**Figure 3.** Cross sections of the PVC/PS/PEG hollow fibers spun at different PEG concentrations (magnification = 1000 $\times$ ).

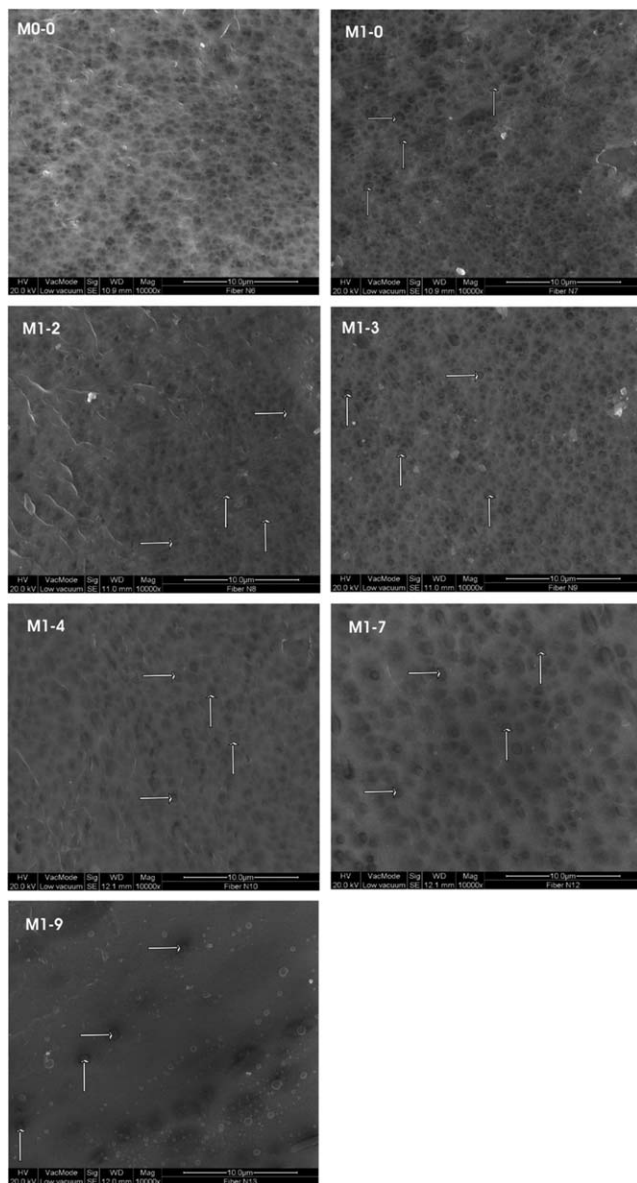


**Figure 4.** Outer surface morphologies of the PVC/PS/PEG hollow fibers spun at different PEG concentrations (magnification = 10,000 $\times$ ).

took place as soon as it was brought into contact with water (the inner coagulant). For this reason, the i.d.'s of the hollow fibers prepared at lower PEG concentrations (from 0 to 4 wt %) were similar to the i.d. of the spinneret. On the other hand, the dope solution viscosity increased with a higher PEG concentration. As a result, the solvent/nonsolvent exchange process was delayed (a kinetic effect). This left the fiber inner layer softer or not completely coagulated. The i.d. increased as a consequence of the inflation because of the bore fluid pressure on the fiber inner wall. A combination of thermodynamic and kinetic effects was also observed by Simone et al.<sup>11</sup> with PVP as an additive for the production of PVDF hollow fibers. The relationship between the coagulation rate and fiber i.d. was also observed in a previous work.<sup>16</sup> In that case, the liquid/liquid demixing rate was delayed because of the use of bore fluids containing different solvent (DMAc) percentages.

The porosity of the produced hollow-fiber membranes, as shown in Table II and Figure 2, decreased from 87.9 to 84.4% with the addition of 1 wt % (M1-0) PS with respect to the pure PVC fibers (M0-0). With the addition of PEG (M1-2 to M1-9), the fiber porosity decreased slightly and, within the limit of experimental error, was constant around 83.3%. This slight reduction of the fiber void fraction could be ascribed to variations in the fiber morphology due to addition of PS and PEG; this reduced the macrovoids, as evidenced in the next section.

### Effect of the PEG Concentration on the Structural Morphology

SEM images of the cross sections of the PVC/PS hollow-fiber membranes prepared with different PEG concentrations, from 0 to 9 wt %, are shown in Figure 3. All of the fibers were made

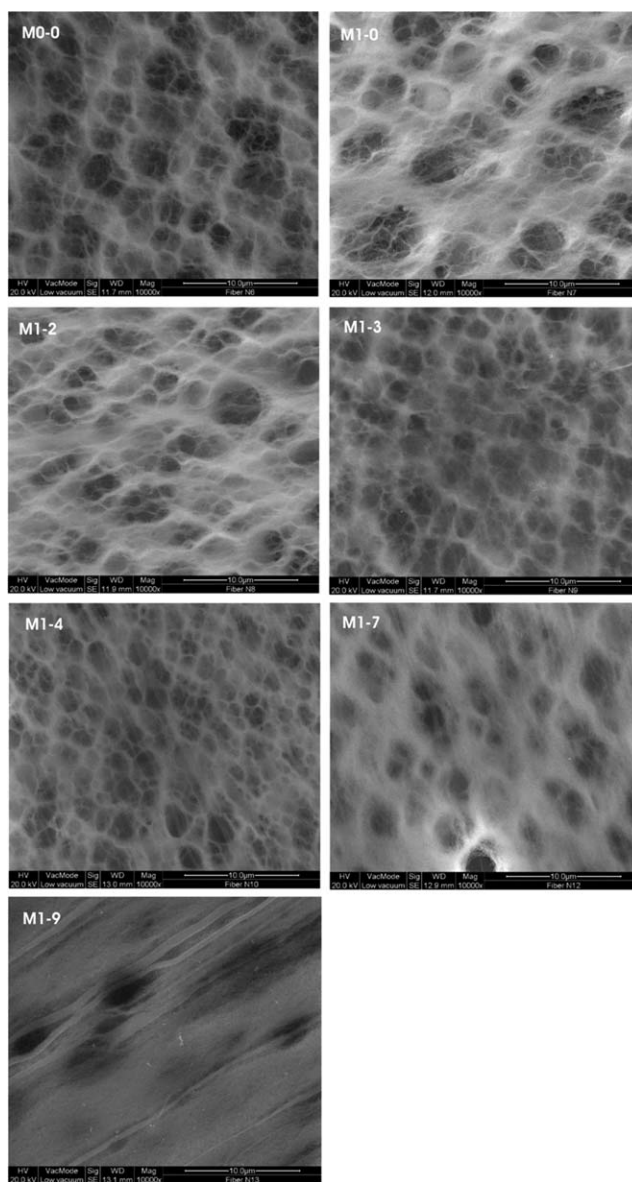


**Figure 5.** Inner surface morphology of the PVC/PS/PEG hollow fibers spun at different PEG concentrations (magnification = 10,000 $\times$ ).

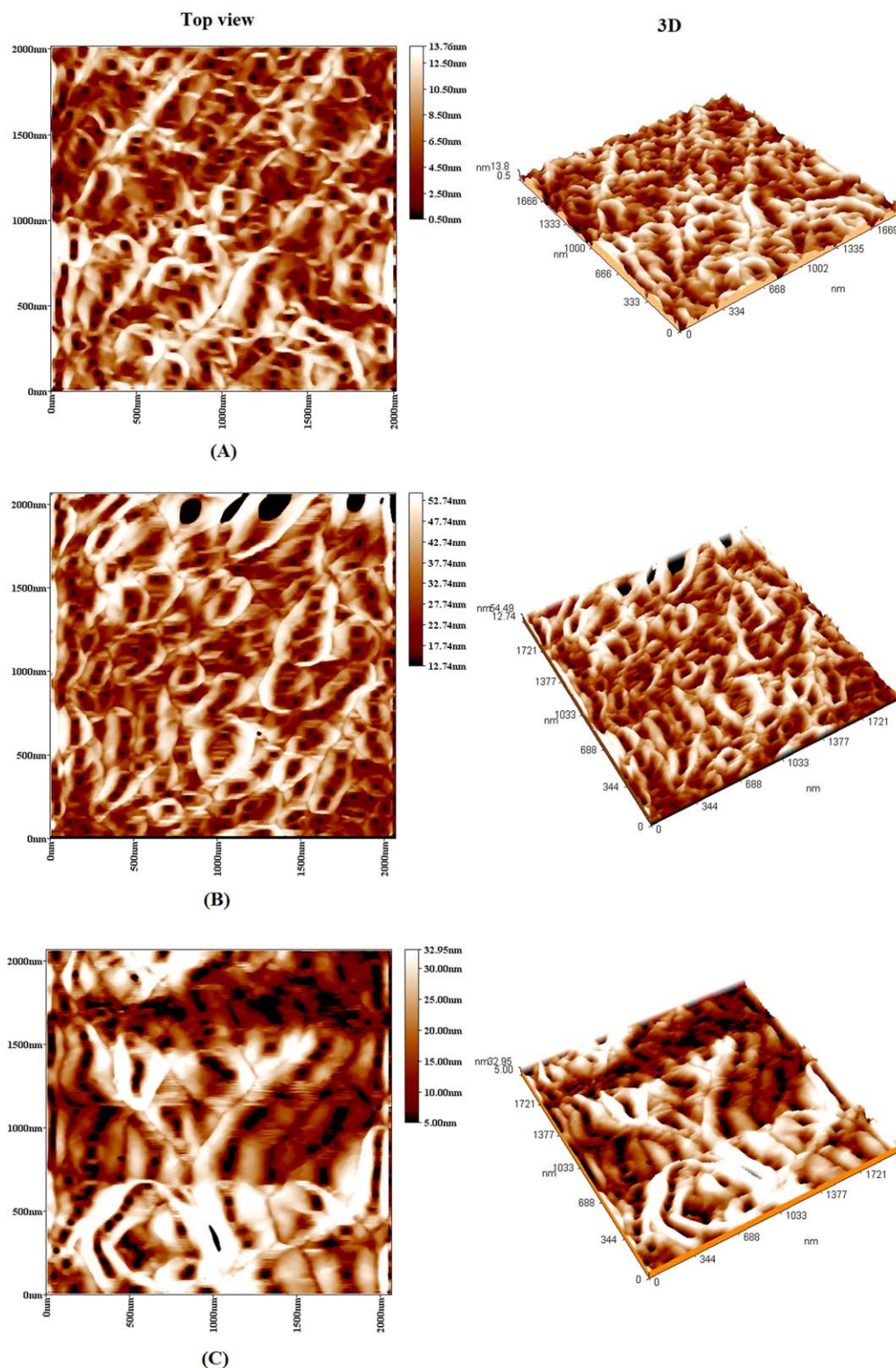


**Figure 6.** Top-view and 3D AFM images of the outer surfaces of the PVC/PS/PEG hollow fibers: (A) pure PVC, (B) 1 wt % PS, (C) 2 wt % PEG, (D) 3 wt % PEG, (E) 4 wt % PEG, (G) 7 wt % PEG, and (H) 9 wt % PEG. [Color figure can be viewed in the online issue, which is available at [wileyonlinelibrary.com](http://wileyonlinelibrary.com).]

up of two layers having a fingerlike structure, namely, layer 1, near the outer surface, and layer 2, near the inner surface, with a thin spongelike layer between them.

For fibers spun without PS and PEG (M0-0), both layers were mainly made up of large tear-drop macrovoids, and the thickness of the two layers was similar. With the addition of 1 wt %

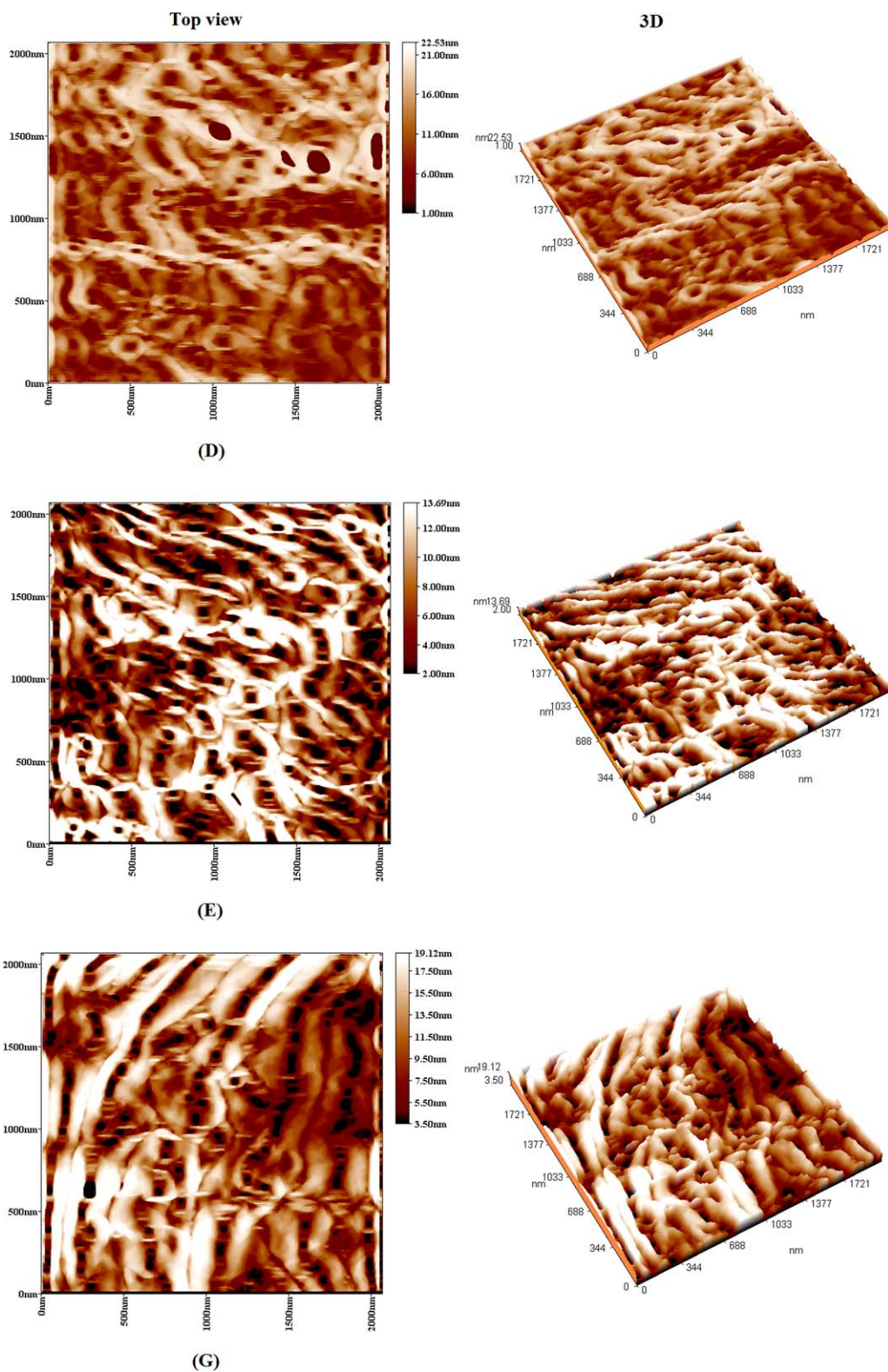


Figure 6. (Continued)

PS (M1-0) to the dope solution, the width of macrovoids in layer 1 (outer surface) was slightly reduced, whereas the morphology of layer 2 seemed unchanged.

With a high PEG concentration in the dope solution (from M1-2 to M1-9), the width of macrovoids in both layers was clearly reduced. The large tear-drop elements were transformed into a

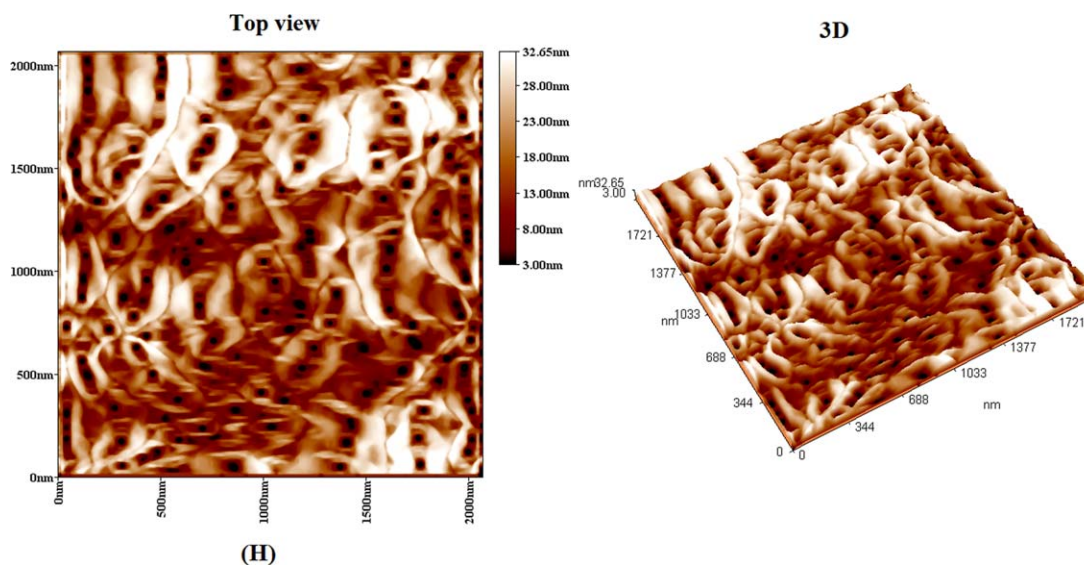


Figure 6. (Continued)

parallel fingerlike structure. This effect was more pronounced for layer 1. Moreover, we also observed that the thickness of both layer decreased, but the effect was much more evident for layer 1 (outer surface).

These changes in the hollow-fiber membrane morphology could be also explained by the coagulation rate and, in particular, the effect of the additive concentration. As already observed in the previous section, the effect of PEG on the fiber coagulation rate arose from an interplay between thermodynamic and kinetic factors. In general, it is widely known that water is a strong nonsolvent for PVC; this means that coagulation takes place quickly when the polymer solution is brought into contact with water. PEG is a water-soluble nonionic surfactant and has strong affinity for water. As a result, when PEG is used as an additive, the nonsolvent diffusion in the polymeric dope is enhanced, and hence, the liquid/liquid demixing rate and coagulation should be faster. Vice versa, with increased PEG concentration in the dope solution, the viscosity increases, and hence, the solvent/nonsolvent exchange can be delayed. This is also in agreement with Simone et al.<sup>11</sup> with regard to PVP

thermodynamic and kinetic effects on the morphology of PVDF hollow-fiber membranes. Large fingerlike macrovoids are generally formed when the coagulation process is fast,<sup>19</sup> whereas a slower coagulation rate results in a porous spongelike structure. At a low concentration of PEG in the dope solution, the thermodynamic driving force plays a major role in solution demixing, inducing the demixing enhancement, corresponding to the acceleration of phase separation due to the PEG additive effect. In fact, tear-drop elements could be still observed for PEG concentrations up to 3–4 wt %; this confirmed the fast coagulation rate, in agreement with reduced fiber i.d.'s observed previously. At higher PEG concentrations, the mutual diffusion was inhibited because of the increase in the dope viscosity, which affected the exchange between water and DMAc during the phase inversion. In this way, the phase separation time increased, and demixing was delayed. Under such delayed demixing conditions, an inhibition of macrovoid formation could be expected.<sup>19</sup>

Therefore, we concluded that although at low PEG concentrations, the macrovoids formation could be slightly enhanced (thermodynamic effect), at higher PEG concentrations, because of the increased viscosity of the dope, the solvent/nonsolvent mutual diffusion was delayed (a kinetic effect), and the macrovoid formation was suppressed. This was in agreement with the reduction of the fibers' overall void fraction observed previously.

The outer and inner surface morphology of the hollow-fiber membranes spun from different ratios of PEG are shown in Figures 4 and 5, respectively. We noticed that the outer surface of the hollow-fiber membrane prepared from pure PVC without PS had an open-cellular morphology [Figure 4(M0-0)], whereas the outer surfaces of the PVC hollow fibers with PS were rough. Spherical particles were observed on the outer surface of the fibers spun from dopes containing 1 wt % PS, as indicated by arrows in the SEM images [from Figure 4(M1-0) to 4(M1-9)]. As already observed in a previous work,<sup>1</sup> these were PS particles, which debonded from the matrix because of incompatibility of the PVC/PS blends.

**Table III.** Mean Pore Size and  $R_a$  Values of the Outer Surface of the PVC/PS/PEG Hollow-Fiber Membranes

Membrane code	Mean pore size (outer surface; nm)	Outer surface roughness (2065 × 2065 nm <sup>2</sup> )		
		$R_a$ (nm)	$R_{ms}$ (nm)	$R_{max}$ (nm)
M0-0	85.71	2.55	2.99	11
M1-0	94.09	10	11.7	40.9
M1-2	120.51	8.15	9.28	27.7
M1-3	121.75	4.04	4.7	17.2
M1-4	137.76	3.55	4.03	11.7
M1-7	182.50	4.25	4.89	15.1
M1-9	184.16	7.12	8.31	29.3



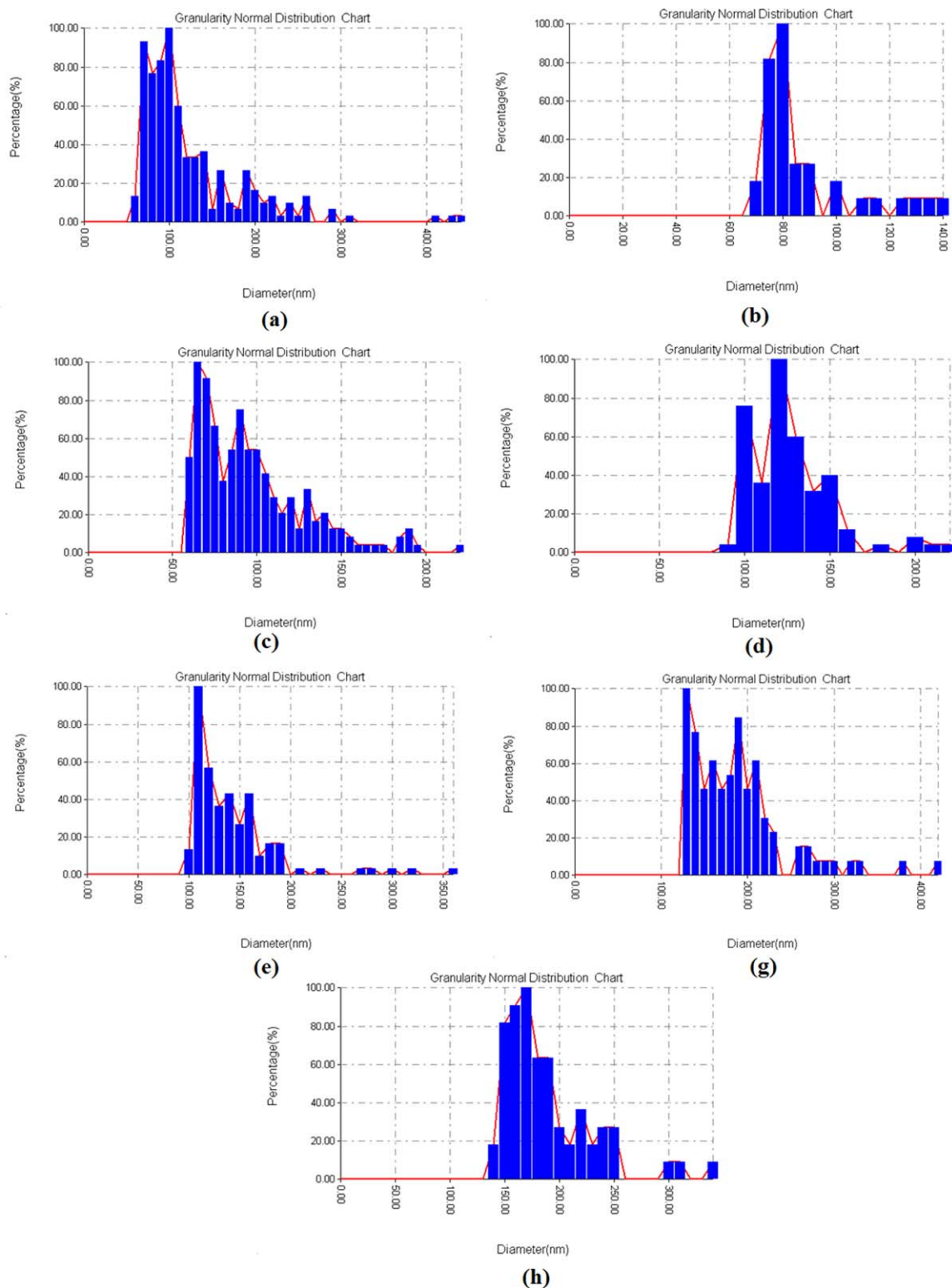


**Figure 7.** Pore size normal distribution of the of the outer surface of the PVC/PS/PEG hollow-fiber membranes: (a) M0-0, (b) M1-0, (c) M1-2, (d) M1-3, (e) M1-4, (g) M1-7, and (h) M1-9. [Color figure can be viewed in the online issue, which is available at [wileyonlinelibrary.com](http://wileyonlinelibrary.com).]

As shown in Figure 5, we noticed that the pore size of the fibers' inner surfaces decreased with an increase in the PEG concentration in the dope solution from 0 to 4 wt % (from M1-0 to M1-4).

Although with a further increase in the PEG concentration in the dope solution from 7 to 9 wt % (from M1-7 to M1-9), the pore size increased with a lower pore density. This could be explained by

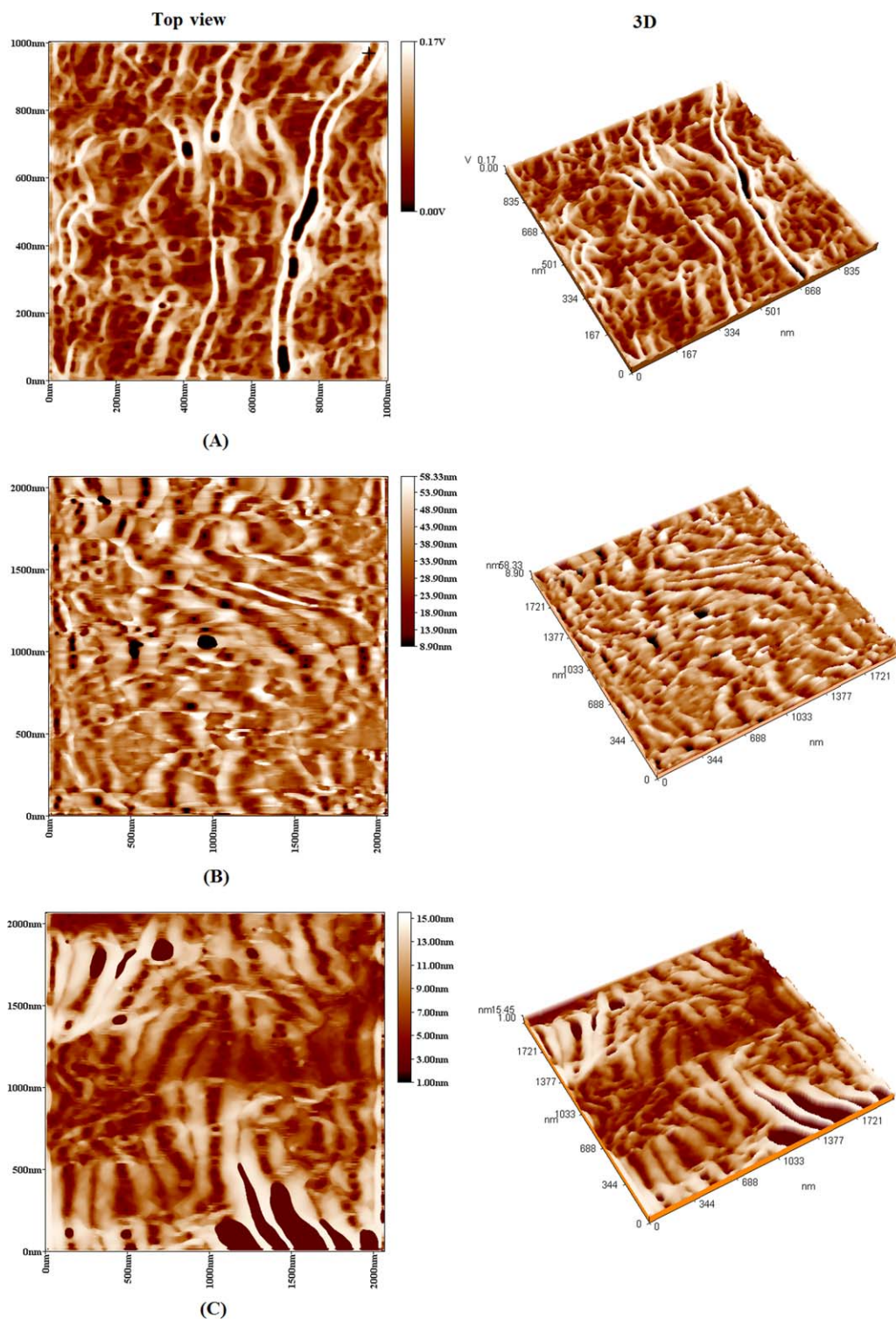


**Figure 8.** Top-view and 3D AFM images of the inner surfaces of the PVC/PS/PEG hollow fibers: (A) pure PVC, (B) 1 wt % PS, (C) 2 wt % PEG, (D) 3 wt % PEG, (E) 4 wt % PEG, (G) 7 wt % PEG, and (H) 9 wt % PEG. [Color figure can be viewed in the online issue, which is available at [wileyonlinelibrary.com](http://wileyonlinelibrary.com).]

the PEG effect on the coagulation rate, which influenced the membrane pore size. As observed previously, the addition of small PEG percentages promoted phase inversion and resulted in a smaller pore size. Further increases in the PEG concentration delayed phase

inversion. This behavior was similar to what was observed in a previous work,<sup>16</sup> in which a high solvent amount in the bore fluid produced large pores and reduced the pore density at the inner surface of PVC fibers because of the delayed phase inversion.

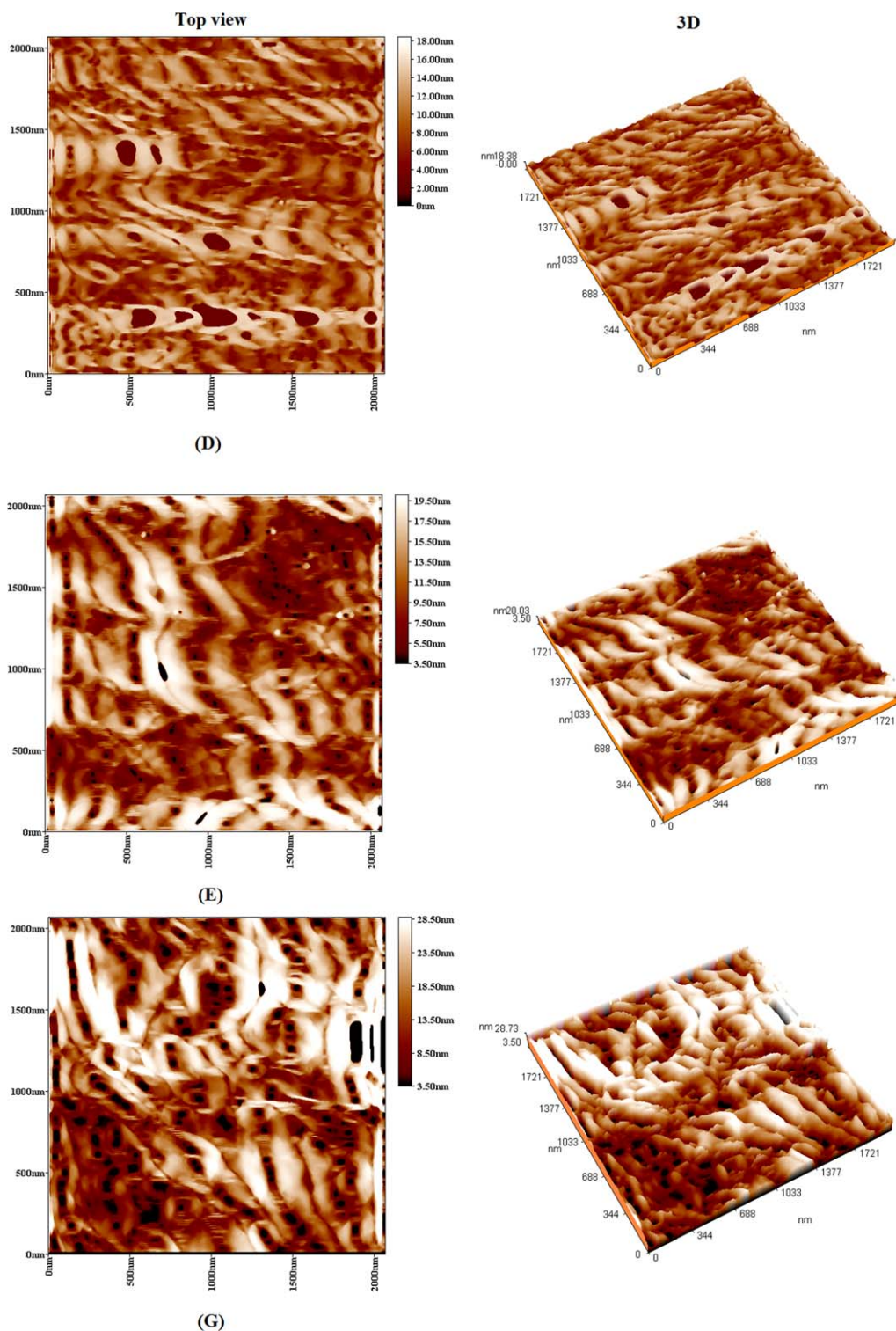


Figure 8. (Continued)

The three-dimensional (3D) and top-view AFM images of the outer surface over an area of  $2065 \times 2065 \text{ nm}^2$  of the PVC-PS hollow-fiber membranes prepared from different PEG-4000 concentrations in the dope solution are shown in Figure 6. We observed that a nodular structure was formed in the outer skin of the PVC-PS hollow fibers with interconnected cavity channels

between the agglomerated areas. However, a significant observation in this study was the new shape of the nodules, called a sea-waves shape; these nodules had a different size, depending on the PEG concentration. In particular, the sea-waves nodule size increased with increasing PEG concentration in the dope solution, as shown in Figure 6. This result has not been reported yet.

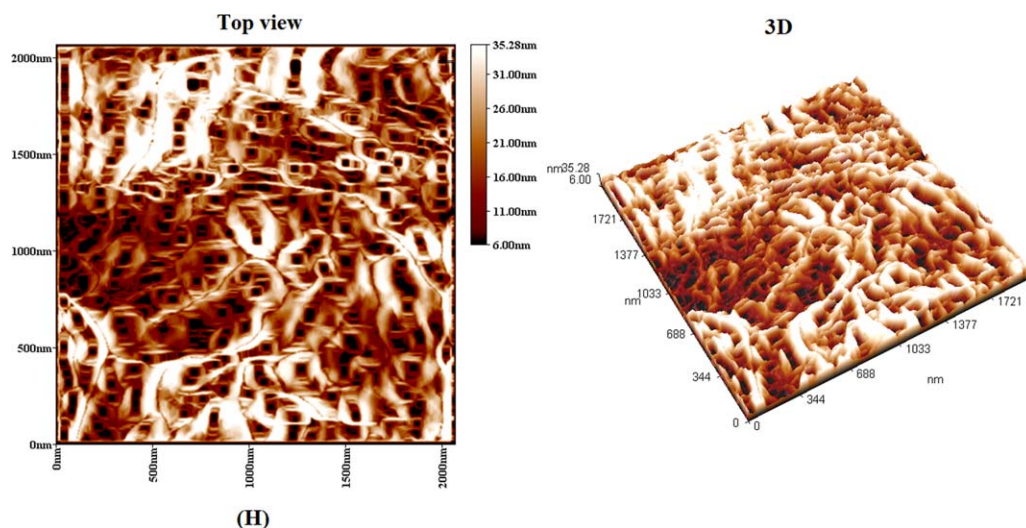


Figure 8. (Continued)

As shown in Figure 6(A–G, top view), the PEG concentration affected the pore size and pore size distribution of the produced hollow fibers. This was due to its effect on the liquid–liquid demixing rate, and it also explained the variations of the membrane morphology, porosity, and pore size observed previously.

The mean pore size, mean roughness ( $R_a$ ; the mean value of the surface relative to the center plane), root mean square of  $Z$  values ( $R_{ms}$ ), maximum roughness ( $R_{max}$ ; vertical distance between the highest peaks and the lowest valleys), and pore size distribution of the outer surfaces of the hollow-fiber membranes were evaluated over an area of  $2065 \times 2065 \text{ nm}^2$  and are shown in Table III and Figure 7. The  $R_a$  values of the hollow fibers prepared from pure PVC were the lowest among all of those of the hollow-fiber membranes prepared in this study. This was due to the higher coagulation rate of the surface during the phase-inversion process. Also, from the results, we observed that the  $R_a$  of the hollow fibers increased greatly with addition of 1 wt % PS in the dope solution.  $R_a$  decreased with increasing PEG concentration from 0 to 4 wt %; a further increase in the PEG concentration resulted in an increase in  $R_a$ . This was attributed to the change in the structural morphology of the hollow

fibers due to the differences in the speed of the liquid–liquid demixing process during the formation of the hollow fibers.<sup>20</sup>

Table III and Figure 7 show the mean pore size and pore size distribution of the PVC/PS/PEG hollow-fiber membranes. It can be seen that the mean pore size increased because of increases in the PEG concentration in the dope solution, and the reason was discussed previously. As shown in Figure 7(A), a wide pore size distribution was obtained for the hollow fibers prepared without PEG as a pore former. With increasing PEG in the polymer solution, the pore size gradually increased with narrow pore size distributions, as shown clearly in Figure 7(B–H).

AFM images of the inner surface over an area of  $2065 \times 2065 \text{ nm}^2$  for hollow-fiber membranes prepared from different PEG-4000 concentrations in the dope solution are shown in Figure 8. We observed a nodular structure in the shape of sea waves was formed at the inner skin of the PVC hollow-fiber membranes. Similarly to what was observed for the outer surface, the sea-waves nodule size increased with increasing PEG concentration in the dope solution (see Figure 8). This phenomenon could also be attributed to the differences in the liquid–liquid demixing process because of the addition of the PEG as a pore former. The inner surface of the hollow fibers prepared from pure PVC had a small pore size, as shown in Figure 8(A, top view). Although the addition of PEG as a pore former in the dope solution resulted in an increase in the pore size of the inner surface, as shown in Figure 8(A–H, top view).

The mean pore size and pore size distribution of the PVC/PS/PEG hollow-fiber membranes are shown in Table IV and Figure 9. We observed that the mean pore size within the limit of experimental error increased with increasing PEG concentration in the dope solution. As shown in Figure 9(A), a wide pore size distribution was obtained for the hollow fibers prepared without PEG as a pore former. With increasing PEG in the polymer solution, the pore size gradually increased with a narrow pore size distribution, as shown in Figure 9(B–H).  $R_a$  of the hollow fiber prepared from pure PVC was very small and improved

**Table IV.** Mean Pore Size and  $R_a$  of the Inner Surface of the PVC/PS/PEG Hollow-Fiber Membranes

Membrane code	Mean pore size (inner surface; nm)	Inner surface roughness ( $2065 \times 2065 \text{ nm}^2$ )		
		$R_a$ (nm)	$R_{ms}$ (nm)	$R_{max}$ (nm)
M0-0	84.64	0.0338	0.04	0.154
M1-0	79.42	8.06	10	49.4
M1-2	117.96	2.95	3.46	12.4
M1-3	139.01	2.89	3.4	13.3
M1-4	119.18	3.84	4.47	16.5
M1-7	234.17	6.77	7.81	25.5
M1-9	203.37	7.95	9.2	29.3

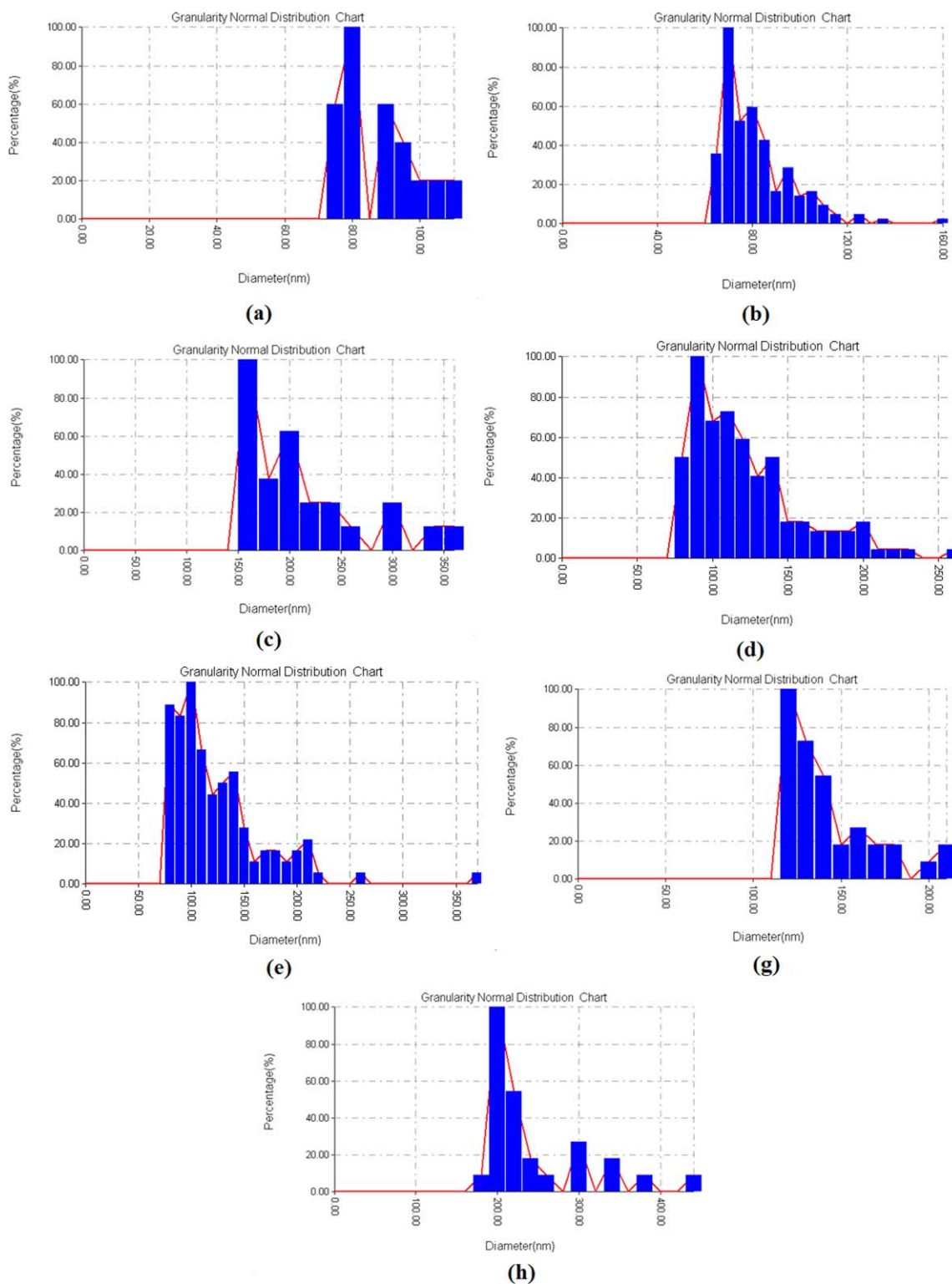


**Figure 9.** Pore size normal distribution of the of the inner surfaces of the PVC/PS/PEG hollow-fiber membranes: (a) M0-0, (b) M1-0, (c) M1-2, (d) M1-3, (e) M1-4, (g) M1-7, and (h) M1-9. [Color figure can be viewed in the online issue, which is available at [wileyonlinelibrary.com](http://wileyonlinelibrary.com).]

greatly with the addition of 1 wt % PS. The addition of 2 and 3 wt % PEG resulted in a decrease in  $R_w$ . A further increase in the PEG concentration up to 9 wt % resulted in an increase in  $R_w$ , as shown in Table IV. This phenomenon was due to the

outflow of PEG from the polymer solution to the nonsolvent (water). The exchange rate increased with increasing amount of PEG in the dope solution, which in turn induced pore formation.

**Table V.** Pure Water Permeation Flux and *R* to PVP (K-90) Values of the PVC/PS/PEG Hollow-Fiber Membranes Produced in This Study

Fiber number	Pure water permeation flux (L m <sup>-2</sup> h <sup>-1</sup> bar <sup>-1</sup> )			PVP <i>R</i> rate (%)
	1.0 Bar	0.8 Bar	0.6 Bar	
M0-0	77	68	52	73.6
M1-0	104	96	82	85.1
M1-2	162	147	130	83.6
M1-3	168	160	132	81.7
M1-4	201	161	149	81.1
M1-7	240	228	187	58.3
M1-9	367	335	302	57.7

Therefore, the results of AFM observations confirmed the mechanism proposed to explain the PEG concentration effects on the membrane morphology, porosity, and surface pore size. In particular, the superposition between the thermodynamic and kinetic effects and the delay of liquid/liquid demixing during coagulation at high PEG concentrations could account for the reduction in macrovoids, decrease in porosity, and increase in surface pore size.

#### Effect of the PEG Concentration on the Separation Performance

The PVC hollow-fiber membranes prepared from the PVC/PS polymeric blends with different PEG concentrations in the dope solution were characterized by the solute transport method with PWP and aqueous solutions containing PVP K-90 ( $M_w = 360$  KDa). PWP and solute *R* (%) values are summarized in Table V.

We observed that the PWP of the PVC/PS hollow-fiber membranes increased from 77 to 367 (L m<sup>-2</sup> h<sup>-1</sup> bar<sup>-1</sup>) with the addition of 1 wt % PS and with increasing percentages of PEG in the polymeric dope. The solute separation factor, evaluated as the *R* value of PVP K-90 ( $M_w = 360$  KDa), increased for small amounts of PEG in the dope and then decreased for high PEG concentrations (7–9 wt %).

As already observed in a previous study,<sup>16</sup> there were five major factors affecting the membrane PWP and *R* values: porosity,

thickness, average pore size, pore size distribution, and pore surface density. The increase in transmembrane water flux was ascribed to the increase in the average pore size of the PVC/PS hollow fibers spun with a high PEG concentration in the dope and the reduction in thickness. The increase in the average pore size observed for M1-7 to M1-9 was also responsible for the reduction in the solute separation factor. The observed results were in agreement with the literature. In previous studies,<sup>15,16</sup> lower solute separation values were found for hollow-fiber membranes having larger pore sizes. Moreover, Wang et al.<sup>21</sup> reported that a decrease in the additive concentration resulted in membranes with a low water solution flux and high *R*.

We concluded that there was an optimum value of PEG concentration in the dope solution (3–4 wt %); this allowed us to improve the performance of the PVC/PS/PEG hollow fibers both in terms of flux and selectivity. Moreover, the slight reduction of membrane void fraction, connected to the reduction of macrovoids, did not affect the membrane performance; this was mainly due to the effect of PEG on the pore size and thickness.

A comparison between the performances of the PVC/PS/PEG hollow-fiber membranes prepared in this study with various membranes selected from the literature and prepared from PVC materials is given in Table VI. We observed that the best combination of PWP and *R* to PVP K-90 was obtained working with a PVC/PS/PEG 14/1/4 w/w blend. Among the PVC hollow fibers reported in the literature, these fibers showed the highest pure water flux, coupled with a high solute separation factor.

#### Effect of the PEG Concentration on the Mechanical Properties

The mechanical properties of the produced hollow fibers were also investigated. The  $R_m$ , ebreak, and EMod values were measured and are presented in Figure 10. The mechanical properties of all of the investigated hollow-fiber membranes were dependent on the PEG concentration in the dope solution. As shown in Figure 10,  $\epsilon_m$  (%) decreased from 73.48 to 58.55% with the addition of 1 wt % PS to the dope solution. The ebreak values then increased from 66.69 to 101.07% with increasing PEG concentration from 2 to 9 wt %. The  $R_m$  slightly increased from 2.98 to 4.42 N/mm<sup>2</sup> with the addition of 1 wt % PS and 2–9 wt % PEG in the dope solution. Also,

**Table VI.** Comparison Between Recently Published Performances of PVC Hollow-Fiber UF Membranes

Membrane material	Thickness (mm)	Pore size ( $\mu$ m)	$\epsilon$ (%)	Membrane configuration	Polymer/solvent composition (wt %)	PWP (L m <sup>-2</sup> h <sup>-1</sup> bar <sup>-1</sup> )	Solute $M_w$ (KDa) and <i>R</i> (%)	Reference
PVC	0.26	—	79.4	Hollow fiber	14/1/85 PVC/PS/DMAc	111.34	PVP, $M_w = 360$ 98.53%	1
PVC/PEG	0.186	—	82.0	Hollow fiber	14/5/81 PVC/PEG-600/DMAc	59	BSA, $M_w = 67$ 99%	3
PVC/PVB	—	—	—	Flat sheet	9/1/90 PVC/PVB/DMAc	197.35	Egg white proteins, $M_w = 43$ 98.59%	12
PVC/PVB	—	—	—	Flat sheet	8/2/90 PVC/PVB/DMAc	129.75	Egg white proteins, $M_w = 43$ 98.98%	12
PVC	0.070	0.13	59.2	Hollow fiber	16/84 PVC/DMAc	153	PVP, $M_w = 360$ 88.5%	15
PVC/PS/PEG	0.27	0.137	83.3	Hollow fiber	16/1/4/79 PVC/PS/PEG/DMAc	201	PVP, $M_w = 360$ 81%	This study

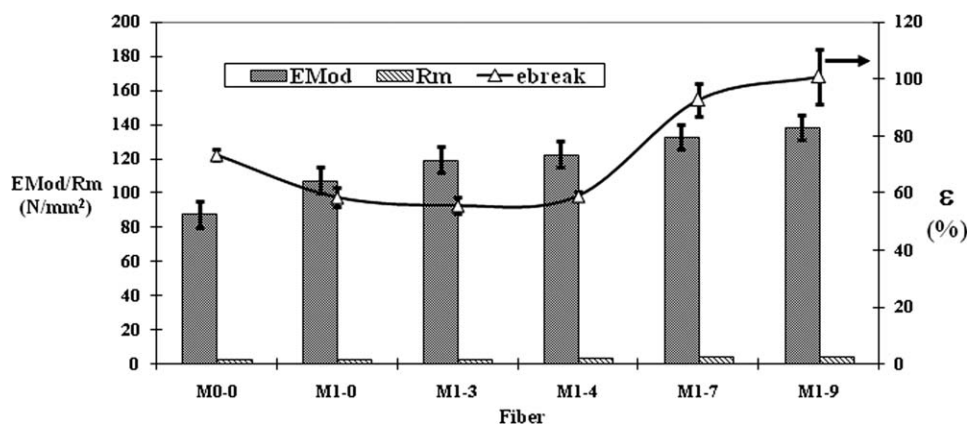


Figure 10. EMod, tensile stress at break, and ebreak of the PVC/PS/PEG fibers produced in this study.

the fiber EMod increased with increasing PS and PEG concentration in the dope solution, and the highest value was obtained for hollow fibers prepared with a 9 wt % PEG concentration (membrane M1-9). This was attributed to a reduction in the tear-drop macrovoid width, especially in the fiber layer near the outer edge (see earlier discussion). This was also consistent with the reduction of fibers overall void fraction observed earlier. The obtained results were in agreement with what was reported in the literature. Xu and Alsally<sup>22</sup> observed that the mechanical properties of membranes increased at higher PEG concentrations in the dope solution. In a previous work,<sup>1</sup> it was also observed that addition of 1 wt % PS to a dope solution increased the EMod of PVC hollow fibers from 97.3 N/mm<sup>2</sup> (14 wt % pure PVC) to 107.48 N/mm<sup>2</sup> (14/1 wt % PVC/PS).

## CONCLUSIONS

Asymmetric PVC/PS hollow-fiber UF membranes were fabricated with a dry/wet phase inversion method. The polymeric dope solutions were prepared from 16 wt % PVC and 1 wt % PS in DMAc. The effects of the PEG concentration (from 0 to 9 wt %) on the membrane morphology, permeability, separation performance, and mechanical properties of the produced fibers were also extensively investigated.

On the basis of the results of this study, the following conclusions were drawn:

1. The i.d. of the PVC/PS/PEG hollow-fiber membranes decreased with increasing PEG concentration up to 4 wt % and increased with PEG concentration up to 9 wt %, although there was no significant effect of PEG on the o.d. because of the air-gap distance (4 cm).
2. The cross-sectional structure of the hollow fibers near the outer edge was changed from a wide and long to a thin and short fingerlike structure with increasing PEG concentration as an additive in the dope solution.
3. The thickness of layer 1 (near the outer edge) decreased with increasing PEG concentration in the dope solution from 2 to 9 wt %.
4. A slight reduction in the fiber porosity, calculated as the average void fraction, was observed as a consequence of macrovoid reduction, despite the use of a hydrophilic pore-forming agent.

5. A new shape of the nodules, denoted as a sea-waves shape, with different sizes in the outer and inner surfaces, was observed. The mean surface roughness of the hollow-fiber membranes decreased with low PEG concentration in the dope solution.
6. The pore size decreased, and the pore density increased up to a PEG concentration of 4 wt %. On the contrary, with further increases in the PEG concentration, the pore size increased, and the pore density decreased on both the inner and outer surfaces of the produced hollow-fiber membranes.
7. The UF experimental results indicated that the PWP increased with PEG concentration, whereas the highest solute  $R$  was observed with 3 and 4 wt % PEG concentration as an additive in the dope solution.
8. The improvement in the transmembrane water flux was mainly connected to the PEG effect on the membrane thickness and pore size, whereas the slight void fraction reduction observed played a minor role.
9. The tensile stress, elongation, and EMod of the PVC/PS/PEG hollow-fiber membranes improved with increasing PEG concentration in the dope solution.

## ACKNOWLEDGMENTS

One of the authors (Q.A.) gratefully thanks the Institute on Membrane Technology, ITM-CNR, and Mariano Davoli (Department of Heart Sciences University of Calabria, Rende, Italy) for the SEM analyses.

## REFERENCES

1. Alsally, Q. *Desalination* **2012**, *294*, 44.
2. Kim, J.; Lee, K. *J. Membr. Sci.* **1998**, *138*, 153.
3. Xu, J.; Xu, Z. *J. Membr. Sci.* **2002**, *208*, 203.
4. Xu, Z.; Alsally, Q. *J. Appl. Polym. Sci.* **2004**, *9*, 3398.
5. Tasselli, F.; Jansen, J. C.; Sidari, F.; Drioli, E. *J. Membr. Sci.* **2005**, *255*, 13.
6. Chou, W.; Yu, D.; Yang, M.; Jou, C. *Sep. Purif. Technol.* **2007**, *57*, 209.
7. Ohya, H.; Shiki, S.; Kawakami, H. *J. Membr. Sci.* **2009**, *326*, 293.

8. Wongchitphimon, S.; Wang, R.; Jiratananon, R.; Shi, L.; Loh, C. H. *J. Membr. Sci.* **2011**, *369*, 329.
9. Arthanareeswaran, G.; Mohan, D.; Raajenthiren, M. *J. Membr. Sci.* **2010**, *350*, 130.
10. Mansourizadeh, A.; Ismail, A. F. *J. Membr. Sci.* **2010**, *348*, 260.
11. Simone, S.; Figoli, A.; Criscuoli, A.; Carnevale, M. C.; Rosselli, A.; Drioli, E. *J. Membr. Sci.* **2010**, *364*, 219.
12. Peng, Y.; Sui, Y. *Desalination* **2006**, *196*, 13.
13. Khayet, M.; Garcia-Payo, M. C.; Alsalhy, Q.; Zubaidy, M. A. *J. Membr. Sci.* **2009**, *330*, 30.
14. Jones, C. A.; Gordeyev, S. A.; Shilton, S. *J. Polymer* **2011**, *52*, 901.
15. Alsalhy, Q.; Algebory, S.; Alwan, G. M.; Simone, S.; Figoli, A.; Drioli, E. *Sep. Sci. Technol.* **2011**, *46*, 2199.
16. Alsalhy, Q. F.; Rashid, K. T.; Noori, W. A.; Simone, S.; Figoli, A.; Drioli, E. *J. Appl. Polym. Sci.* **2012**, *124*, 2087.
17. Feng, C.; Shi, B.; Li, G.; Wu, Y. *J. Membr. Sci.* **2004**, *237*, 15.
18. Brandrup, J.; Immergut, E. H.; Polymer Handbook, 3rd ed.; Wiley: New York, **1989**.
19. Smolder, C. A.; Reuver, A. J.; Boom, R. M.; Wienk, I. M. *J. Membr. Sci.* **1992**, *73*, 259.
20. Chung, T. S.; Qin, J. J.; Huan, A.; Toh, K. C. *J. Membr. Sci.* **2002**, *196*, 251.
21. Wang, D.; Li, K.; Teo, W. K. *J. Membr. Sci.* **1999**, *163*, 211.
22. Xu, Z.; Alsalhy, Q. F. *J. Appl. Polym. Sci.* **2004**, *91*, 3398.